Pharm Res (2015) 32:665–679
DOI 10.1007/s11095-014-1494-0

RESEARCH PAPER

The Characterization of the Human Nasal Epithelial Cell Line RPMI 2650 Under Different Culture Conditions and Their Optimization for an Appropriate *in vitro* Nasal Model

Mateja Erdani Kreft • Urška Dragin Jerman • Eva Lasič • Tea Lanišnik Rižner • Neli Hevir-Kene • Luka Peternel • Katja Kristan

Received: 11 March 2014 / Accepted: 15 August 2014 / Published online: 22 August 2014

ABSTRACT

Purpose The further characterization of the cell line RPMI 2650 and the evaluation of different culture conditions for an *in vitro* model for nasal mucosa.

Methods Cells were cultured in media MEM or A-MEM at air-liquid (A-L) or liquid-liquid (L-L) interfaces for 1 or 3 weeks. Different cryopreservation methods and cell culture techniques were evaluated with immunolabelling of junctional proteins, ultrastructural analysis using electron microscopy, transepithelial electrical resistance (TEER) measurements, permeation studies with dextran and jacalin, and gene expression profiling of 84 drug transporters.

Results Cell proliferation and differentiation depended on the used medium. The established epithelia expressed occludin, claudin-1, and E-cadherin under all conditions. Cells grown at the A-L interface formed more layers and exhibited a higher TEER and lower dextran and jacalin permeability than at the L-L interface, where cells morphologically exhibited a more differentiated phenotype. The expression of ABC and SLC transporters depended on culture duration and interface.

Conclusions The RPMI 2650 cells form a polarized epithelium resembling nasal mucosa. However, different culture conditions have a significant effect on cell ultrastructure, barrier integrity, and gene expression, and should be considered when using this cell line as an *in vitro* model for drug permeability studies and screening of nasal drug candidates.

KEY WORDS drug transporters · microscopy · nasal epithelial cell model · permeability · TEER

ABBREVIATIONS

A	Surface area
ABC	ATP-binding cassette
A-L	Air-liquid interface
c_0	Initial donor concentration
dQ/dt	Flux of dextran-FITC or jacalin-fluorescein across the RPMI 2650 cell barrier
L-L	Liquid-liquid interface
P_{app}	Apparent permeability coefficient
SEM	Scanning electron microscopy
SLC	Solute carrier
TEER	Transepithelial electrical resistance
TEM	Transmission electron microscopy
TJ	Tight junction

INTRODUCTION

The nasal administration of aerosol therapeutics is becoming an appealing alternative in drug delivery. This non-invasive method offers higher bioavailability with its avoidance of first-pass metabolism, intestinal efflux transporters, and degradation in the digestive system, as well as a large absorptive surface area, leaky epithelium, and extensive vascularization of the nasal cavity, which altogether enable rapid direct transport into the systemic circulation (1–3). The mucosal barrier of the upper respiratory tract includes the nasal cavity, which is the first exposure site to inhaled substances, and is largely regulated by the tight junctions (TJs) of epithelial cells (4).

Electronic supplementary material The online version of this article (doi:10.1007/s11095-014-1494-0) contains supplementary material, which is available to authorized users.

M. E. Kreft • U. D. Jerman • E. Lasič
Institute of Cell Biology, Faculty of Medicine, University of Ljubljana
Ljubljana, Slovenia

L. Peternel • K. Kristan
Lek Pharmaceuticals, d.d., Sandoz Development Center Slovenia
Ljubljana, Slovenia

T. Lanišnik Rižner • N. Hevir-Kene • K. Kristan (✉)
Institute of Biochemistry, Faculty of Medicine, University of Ljubljana
Ljubljana, Slovenia
e-mail: katja.kristan@sandoz.com

Because the airway epithelium is a protective interface, its transepithelial transport properties must be assessed in order to evaluate its suitability for drug delivery (5).

In vitro models of nasal mucosa have been utilized using excised tissue, primary cell cultures, or immortalized cell lines (3). However, excised human tissue is hard to obtain and using animal tissues introduces problematic species differences (6). On the other hand, *in vitro* cell cultures increase the possibility of using human tissue and reduce time-consuming, expensive, and ethically controversial animal studies in addition to offering quick assessment of drug biopharmaceutics (2). Nevertheless, primary cell cultures have disadvantages such as limited access to tissues, complex isolations, short lifespans, considerable heterogeneity within and between cultures, and uncertain reproducibility (3, 6). Additionally, the variations of different domains and cell types of the nasal cavity create issues in selecting the precise area of excision (6). Last but not least, the financial expenditures of human airway epithelial cells often hinder their use in experimentation (5). On the contrary, immortalized cell lines exhibit genetic homogeneity, provide reproducibility of results, and are easily maintained in culture (3, 7, 8). Epithelial cell lines are the most utilized for drug transport studies, yet there is a lack of cell lines that mimic nasal epithelium (9).

So far, the only human cell line used for nasal drug transport studies has been RPMI 2650 (9). This cell line originates from an anaplastic squamous cell carcinoma of the nasal septum and has displayed consistent growth and high stability throughout continued culturing *in vitro* with no alteration to the normal diploid karyotype (10, 11). The RPMI 2650 cell line requires a shorter culture time to reach confluence than human primary nasal cell cultures and is therefore considered superior (6). RPMI 2650 cells produce mucoid material on their cell surfaces similar to normal human nasal epithelium (10, 12) and form an enzymatic metabolic barrier similar to that of excised human nasal tissue (13). RPMI 2650 cells also form polarized epithelium of cells interconnected with the cell junction proteins ZO-1, occludin, claudin-1, E-cadherin, and β-catenin (9, 12) and have been shown to develop microvilli (12, 14, 15). The RPMI 2650 model has exhibited an organotypic permeation barrier consisting of a tight homogenous cell multilayer with a transepithelial electrical resistance (TEER) closer to physiological conditions than primary cell cultures, and permeation coefficients in the same range as human nasal mucosa (3). Similarly another study demonstrated that the RPMI 2650 model exhibits permeabilities comparable to that of excised nasal mucosa (16).

Nevertheless, not enough studies of the characterization of the cell line have been performed and its suitability as an *in vitro* model is still under question. A standardized culturing system under optimal conditions is necessary to establish a valid *in vitro* nasal cell culture model with differentiated cells and developed TJs to study the permeability and metabolic barrier of nasal epithelium. For this reason, we have further characterized and optimized the RPMI 2650 cell line model using different culturing conditions, immunolabeling of cell junction protein expression, ultrastructural analysis using scanning electron microscopy (SEM) and transmission electron microscopy (TEM), TEER measurements of barrier integrity, permeation studies of barrier function, and screening for the expression of various drug transporters.

MATERIALS AND METHODS

Cell Culture

The RPMI 2650 cells were obtained from the European Collection of Cell Cultures, Health Protection Agency (Cat. No. 88031602, Lot No. 10D028) and used from passages 11 to 19. The cells were maintained either in MEM (Eagle's Minimum Essential Medium, Gibco, Invitrogen, Life technologies, Austria) supplemented with 0.11 g/L sodium pyruvate, 4 mM GlutaMAX™, and 10% FBS, or in A-MEM (Advanced Minimum Essential Medium, Gibco) supplemented with 4 mM GlutaMAX™ and 2.5% FBS. The cell cultures were maintained at 37°C in a >95% humidified atmosphere of 5% CO_2 in air with media changes on alternate days. Once 80–100% confluent, the cells were harvested. The cells were detached with TripLE™ Select (Gibco), collected, and centrifuged at 200 g for 5 min at room temperature. The cell pellet was then resuspended in culture medium, the cells were counted with a haemocytometer and their viability was assessed with the Trypan blue method. The cells were seeded at densities 1×10^5 cells/cm^2, 2×10^5 cells/cm^2, 4×10^5 cells/cm^2, 6×10^5 cells/cm^2, and 1×10^6 cells/cm^2 onto polystyrene Tissue Culture Flasks (TPP, Switzerland) and their proliferation and viability was assessed.

For the evaluation of RPMI 2650 cell models on different substrates and interfaces, the cells were seeded onto three different polyethylene terephthalate porous membranes (BD Falcon Cat. No. 353090, 353180; Corning, HRS Transwell-24-Systems Cat. No. 3379; and Milipore, Millicell®-24 Cat. No. PSRP 010 R1) with the established optimal seeding density of 6×10^5 cells/cm^2. To establish the liquid-liquid (L-L) interface, an appropriate volume of culture medium was added to both the apical and basal compartments, whereas for the air-liquid (A-L) interfaces the culture medium was removed from the apical compartment after the first day of cell seeding. The RPMI 2650 epithelial models on porous membranes were maintained in culture for 1 or 3 weeks.

Cryopreservation

When the RPMI 2650 cells reached confluence in a 75 cm^2 Tissue Culture Flask (TPP), they were harvested as described

above and resuspended into a cryovial (TPP) in either FBS: DMSO (9:1), FBS:medium:DMSO (2:7:1), or glycerol:medium (1:1). They were then kept for 1 h at 4°C, followed by 3 h at −20°C, and finally transferred and stored at −80°C or in liquid nitrogen at −196°C. After 3 weeks the cells were quickly thawed in a water bath at 37°C, centrifuged at 200 g for 5 min at room temperature, and resuspended. The cells were counted and their viability was assessed with the Trypan blue method. They were then seeded onto Tissue Culture Flasks (TPP) and their proliferation in culture was assessed.

Transepithelial Electrical Resistance Measurements

When the RPMI 2650 cells at the L-L and A-L interfaces reached confluence on the porous membranes (BD Falcon), TEER was measured using an epithelial voltohmmeter (EVOM, WPI) with electrodes (STX2, WPI). To conduct the measurements, culture media (0.5 mL) was added to the apical compartment of the A-L interface for 3 min. TEER was measured 5 days a week for 1 month. The measured TEER values were corrected by subtracting the mean resistance of blank porous membranes [150 Ωcm^2].

Transmission Electron Microscopy

RPMI 2650 cells seeded at a density of 6×10^5 cells/cm^2 and cultured at either interface in either medium on porous membranes (BD Falcon) for 3 weeks were fixed with 4% (*w*/*v*) formaldehyde and 2.5% (*v*/*v*) glutaraldehyde in 0.1 M cacodylate buffer, pH 7.4 for 2 h 45 min. The fixation was followed by overnight rinsing in 0.33% sucrose in 0.1 M cacodylate buffer and post-fixation in 1% (*w*/*v*) osmium tetroxide and 3% potassium ferrocyanide for 1 h at 4°C. Afterwards, the samples were incubated in 0.3% thiocarbohydrozide for 5 min at room temperature and in 1% osmium tetroxide for 20 min at 4°C. The samples were then dehydrated in a graded series of ethanol and embedded in Epon (Serva Electrophoresis, Heidelberg, Germany). Epon semithin sections were stained with 1% toluidine blue and 2% borate in distilled water and observed with a Nicon Eclipse TE microscope. Ultrathin sections were contrasted with uranyl acetate and lead citrate and observed with a transmission electron microscope (Philips CM100).

Scanning Electron Microscopy

RPMI 2650 cells seeded at a density of 6×10^5 cells/cm^2 and cultured at either interface in either medium on porous membranes (BD Falcon) for 3 weeks were fixed in 2% (*w*/*v*) formaldehyde and 2.5% (*v*/*v*) glutaraldehyde in 0.1 M cacodylate buffer, pH 7.4 for 3 h at 4°C. The fixation was followed by overnight rinsing in 0.2 M cacodylate buffer and post-fixation in 1% (*w*/*v*) osmium tetroxide for 1 h at 4°C. After dehydration, the models were dried at the critical point, spattered with gold, and examined with a Jeol JSM 840A scanning electron microscope.

Immunofluorescence

The RPMI 2650 cells seeded at a density of 6×10^5 cells/cm^2 and cultured at either interface in either medium on porous membranes (BD Falcon) for 3 weeks were fixed in cold (−30°C) 100% ethanol for 25 min at room temperature and then washed with PBS (phosphate buffered saline) for 15 min. The cells were first blocked with 1% BSA (bovine serum albumin) in PBS, and then incubated with the primary antibodies: rabbit polyclonal anti-occludin (Zymed-Life Technologies, 71–1500), rabbit polyclonal anti-claudin-1 (Zymed-Life Technologies, 71–7800), or mouse monoclonal anti-E-cadherin (BD Transduction Laboratories, 610182) overnight at 4°C. All primary antibodies were diluted at 1:20 in 1% BSA in PBS). This was followed by washing in PBS for 30 min and incubation with a secondary antibody (goat anti-rabbit or anti-mouse IgG conjugated to Alexa 488 (Invitrogen)) diluted 1:400 in 1% BSA in PBS. The samples were then washed in PBS for 30 min, transferred onto slides and mounted with DAPI-Vectashield (Vector Laboratories, Burlingame, CA, USA). For the negative controls primary antibodies were omitted. The samples were viewed with a fluorescence microscope AxioImager.Z1 with an Apotome attachment (Carl Zeiss MicroImaging GmbH, Heidelberg, Germany).

Permeability Studies

RPMI 2650 cells were seeded with a density of 6×10^5 cells/cm^2 onto porous membranes (Millicell-24 Cell Culture Insert, 1 μm pore size) and cultured at either interface in either medium. The permeability through all cell layers of the different models was assessed using the markers dextran, conjugated to fluorescein isothiocyanate (Invitrogen, Cat. No. D22910, MW 10000), and jacalin, conjugated to fluorescein (Vector Laboratories, Cat. No. FL-1151). After 3 weeks in culture, 200 μL of dextran-FITC [1 mg/mL] or jacalin-fluorescein [20 μg/mL], diluted in culture medium, were added to the apical compartment, whilst 800 μL of culture medium was in the basal compartment. Additionally, permeability studies through porous membranes without cells were performed. The models were returned to the incubator and samples were taken from the basal compartment at 30-min intervals up to 3 h.. The amounts of dextran-FITC and jacalin-fluorescein in the basal samples were determined using a microtiter plate reader (Infinite M1000, Tecan). The amount of diffused marker was calculated from a calibration curve for each marker. The apparent permeability coefficient P_{app} (17) was calculated from the linear plot of marker

accumulated in the basal compartment, i.e. receiver side *versus* time using the following equation:

$$P_{app} = \frac{dQ}{dt} / (c_0 \times A)$$

where dQ/dt is the flux [μg/s] of dextran-FITC or jacalin-fluorescein across the RPMI 2650 cell barrier, c_0 is the initial donor concentration [μg/mL], and A is the surface area [cm^2].

Assessment of Fluorescently Labeled Vesicles

After the RPMI 2650 models were incubated for 2 h with dextran-FITC or jacalin-fluorescein, the models were fixed in 4% paraformaldehyde for 20 min. The samples were then washed in PBS for 15 min and mounted onto slides with DAPI-Vectashield (Vector Laboratories, Burlingame, CA, USA). The RPMI 2650 models were examined with the AxioImager.ZI microscope with an Apotome attachment (Zeiss) and optical sections of all samples were made. The number of fluorescent vesicles was assessed using ImageJ FociPicker software, using the first 40 optical sections in all the samples.

qPCR Assay

The Human Drug Transporters RT^{2}Profiler™ PCR array (PAHN070, SABiosciences, A Qiagen Company) was used to perform qPCR assays. The array enables the assessment of 84 human drug transporter genes, including 29 ATP-binding cassette transporters, 46 solute carrier transporters, 9 transporters from other families, as well as the five reference genes *B2M*, *HPRT1*, *RPL13A*, *GAPDH*, and *ACTB* (see Fig. 9 and Supplemental Table I for a list of all genes).

The RPMI 2650 cells were cultivated on porous membranes (BD Falcon) at either interface in A-MEM medium for 1 or 3 weeks. The total RNA was isolated using the Qiazol Lysis Reagent (Qiagen) and the RNA samples were dissolved in RNase-free water. The RNeasy Mini Kit (Qiagen) was used for RNA purification and the samples were then treated with RNase-free DNase Set (Qiagen). The purity and quality of extracted RNA were analyzed with the Agilent 2100 Bioanalyzer using the RNA 600 Nanokit. The RNA samples had an average RNA Integrity Number of 8.77 ± 0.57, which demonstrates that the RNA was of good quality. Reverse transcription was carried out using a RT^2 First Strand Kit (Qiagen). The RT Profiler PCR Array System and RT^{2}qPCR SYBR Green Master Mix were used for real-time PCR (40 cycles). All the quality control parameters for genomic DNA contamination, reverse transcription, and PCR reaction success were within the recommended limits. The effect of culturing at different interfaces and culture time were assessed. Genes that differed more than four-fold were considered significant. Data analysis was performed using the ΔC_q method, where the ΔC_q value is normalized to the geometric mean of all five reference genes (*B2B*, *HPRT1*, *RPL13A*, *GAPDH*, and *ACTB*).

Statistical Analysis

The results were compared using a Student *t*-test and expressed as mean ± standard error (SE); p values less than 0.05 were considered statistically significant.

RESULTS

Cell Seeding and Proliferation

The RPMI 2650 cell line is most often cultured in MEM. In this study, we observed the effect of MEM and A-MEM on RPMI 2650 cell cultures. A-MEM is a newer medium that allows normal cell culturing with reduced serum supplementation, which renders larger reproducibility. Cell cultivation was successful in both A-MEM and MEM and cell proliferation was proportional to the seeding density. Several different seeding densities were tested and the density 6×10^5 cells/cm^2 proved to be most efficient, with fast proliferation and confluence being reached in 1 week (Fig. 1). Cell proliferation was faster in A-MEM than in MEM. During cell lifting, RPMI 2650 cells were observed to round and lift quicker (10–15 min) in A-MEM than in MEM (15–20 min), suggesting better cell-cell contacts in MEM. Cell viability remained very high in both media MEM and A-MEM (99.3 ± 0.15% and 99.2 ± 0.10%, respectively) until the third week and then dropped to 96.4% in MEM and 91.5% in A-MEM. The larger drop in cell viability in A-MEM might be due to the larger number of cells and shortage of nutrients. Additionally, different substrates for culturing cells were tested and cell cultivation was demonstrated to be similar on polystyrene flasks (TPP, BD Falcon) as well as on polyethylene terephthalate porous membranes (BD Falcon, Corning, and Millipore), regardless of pore size.

Cell Viability After Cryopreservation

RPMI 2650 cells were cryopreserved for 3 weeks with six different methods, after which cell viability and proliferation were assessed in MEM and A-MEM. The cell viabilities after cryopreservation in FBS:DMSO (9:1) at −80°C or −196°C did not differ significantly (73% and 78%, respectively) nor did cell proliferation differ after thawing (Fig. 2). However, cells cultured in A-MEM proliferated noticeably faster than in MEM, reaching 90% confluence in A-MEM and only 50% confluence in MEM after 2 weeks (Fig. 2). The cell viabilities

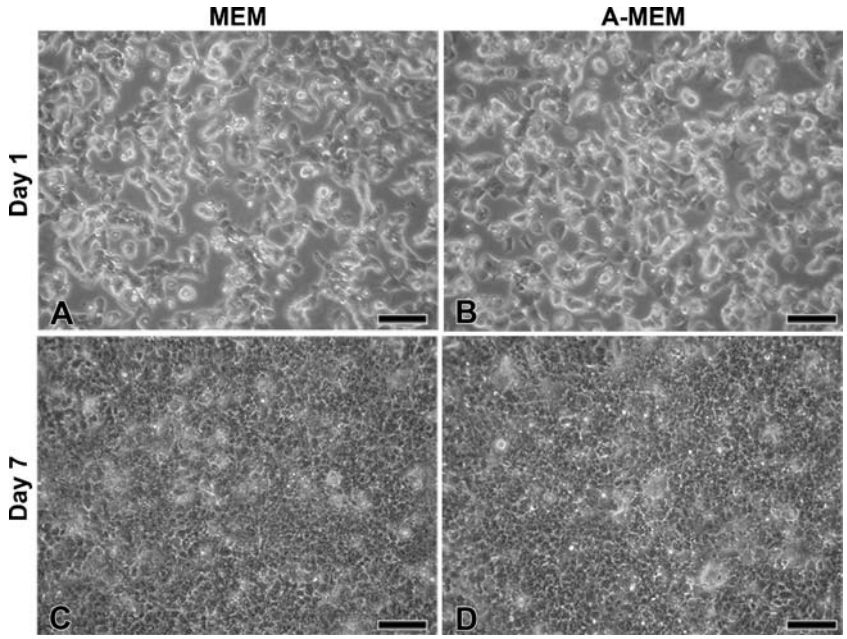

Fig. 1 RPMI 2650 cell cultures in media MEM and A-MEM seeded with a density of 6×10^5 cells/cm^2 on day 1 (**a**, **b**) and 7 (**c**, **d**). Scale bars: 100 μm.

after cryopreservation in FBS:medium:DMSO (2:7:1) at −80°C or −196°C did not differ significantly (75% and 81%, respectively). However, cell proliferation was better after cryopreservation in FBS:medium:DMSO than in FBS:DMSO (data not shown). Additionally, the suitability of using glycerol as a cryoprotectant was tested and this method yielded 0% viability after 3 weeks.

Histology and Ultrastructure of Different RPMI 2650 Models

RPMI 2650 cells successfully adhere, proliferate, and form multi-layered epithelia on all the porous membranes tested. Cells at the A-L interface formed an epithelium with many layers (up to 10 cell layers in MEM and 20 in A-MEM) (Fig. 3). The established epithelium resembled a squamous carcinoma as well as a nasal papilloma in A-MEM. Cells cultured at the L-L interface also formed a multi-layered epithelium, but consisting of only 5–7 cell layers, regardless of the media used. Additionally, necrotic cells in the superficial layers of epithelia were observed, most abundantly in A-MEM at the A-L interface. The models cultured at the L-L interface exhibited a more differentiated phenotype than when cultured at the A-L interface (Fig. 4) and resembled a stratified squamous epithelium.

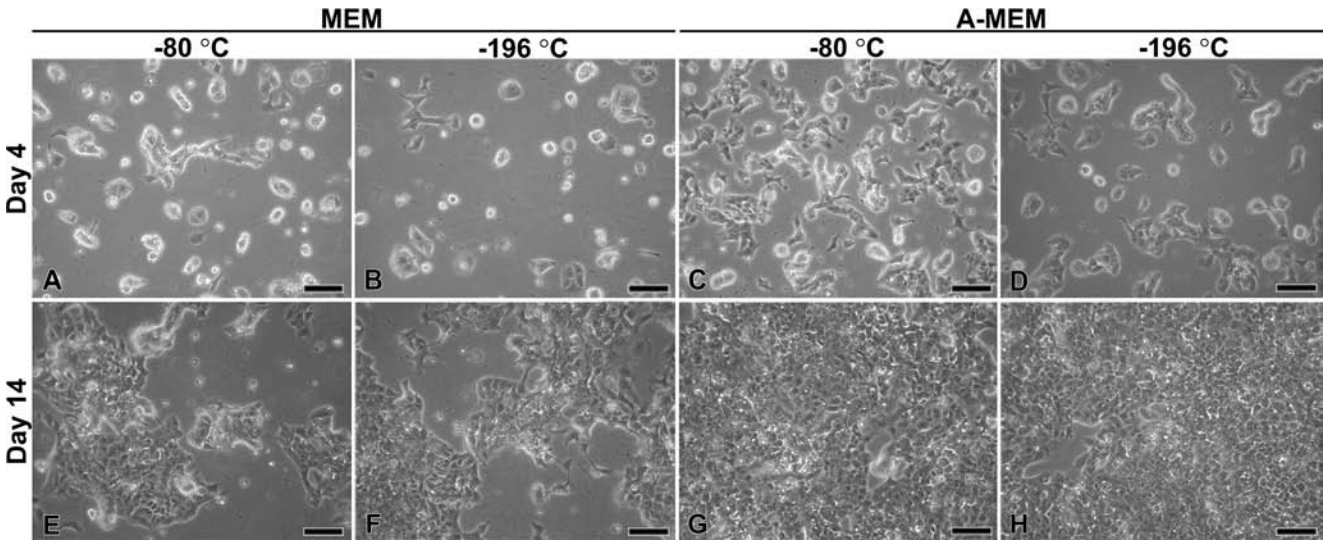

Fig. 2 RPMI 2650 cell proliferation in media MEM (**a**, **b**, **e**, **f**) and A-MEM (**c**, **d**, **g**, **h**) after 3 weeks cryopreservation in FBS:DMSO (9:1) at −80°C or −196°C. Cell seeding density was 2×10^5 cells/cm^2. Note the faster cell proliferation in A-MEM. Scale bars: 100 μm.

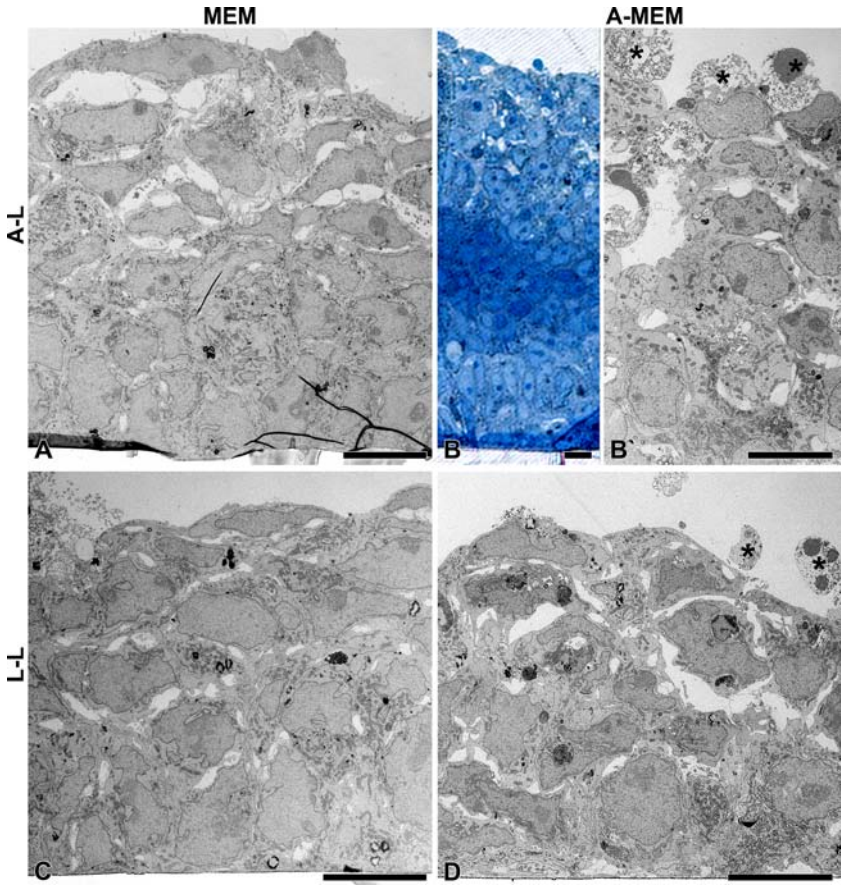

Fig. 3 RPMI 2650 epithelia in media MEM and A-MEM at the A-L and L-L interface after 3 weeks in culture observed with TEM or light microscopy. (**a**, **b**) The most layered epithelia were formed when cells were cultured at the A-L interface, with the highest number of layers formed in A-MEM. On **B′** the superficial layers of epithelia cultured in A-MEM at the A-L interface are shown. Note the necrotic superficial cells (*). (**c**, **d**) The number of cell layers was lower when cultured at the L-L interface, however some necrosis of superficial cells was still observed in A-MEM (*). Scale bars: 10 μm.

In all four models the cells exhibited large intercellular spaces in the superficial layers, whereas the basal layers were tighter (Fig. 5). After 3 weeks at the L-L interface, some of the superficial cells cultured in A-MEM exhibited developed microvilli and cilia-like structures, whereas superficial cells cultured in MEM exhibited less microvilli, but formed more developed cell junctions, which was confirmed with higher mean TER values.

Immunofluorescence of Cell Junction Proteins

The RPMI 2650 models at the L-L interface in both media MEM and A-MEM expressed the TJ proteins occludin and claudin-1 as well as the adherens junction protein E-cadherin (Fig. 6). In cultures established in A-MEM at the L-L interface all three junction proteins were expressed in intermediate and basal cells, however in superficial cells the expression was significantly low or lacking, which confirms the observations with TEM. Occludin was homogenously expressed throughout the cell culture, whereas claudin-1 and E-cadherin were only expressed well in regions with more cell layers. The RPMI 2650 models at the A-L interface in both media MEM and A-MEM also expressed all three cell junction proteins (data not shown).

TEER of the RPMI 2650 Models

The TEER of the established RPMI 2650 models was significantly affected by the culturing conditions. Cultures established in A-MEM proliferated faster and thus reached their maximal TEER faster than cultures established in MEM (in 1 week and 2 to 3 weeks after confluence, respectively). TEER of the models was significantly higher at the A-L interface (41.0 ± 0.9 Ωcm^2 in MEM and 38.3 ± 0.9 Ωcm^2 in A-MEM) than at the L-L interface (30.4 ± 0.5 Ωcm^2 in MEM and 25.2 ± 0.7 Ωcm^2 in A-MEM) (Fig. 7).

Dextran Permeability of the RPMI 2650 Models

To study the integrity of the RPMI 2650 epithelial cell culture model, we used a high molecular weight dextran (MW 10000). The interface of the models had a significant effect on dextran permeability (Fig. 8a). The models cultured at the A-L interface formed the tightest barrier. The tightest barrier was demonstrated to be formed in the models cultured in A-MEM (P_{app} 6.08×10^{-7} cm/s), compared to MEM (P_{app} 8.90×10^{-7} cm/s). Whereas the P_{app} of the cell cultures at the L-L interface were higher than at the A-L interface and similar in both media (9.44×10^{-7} cm/s in A-MEM and 10.0×10^{-7} cm/s in MEM). Permeability of dextran through the

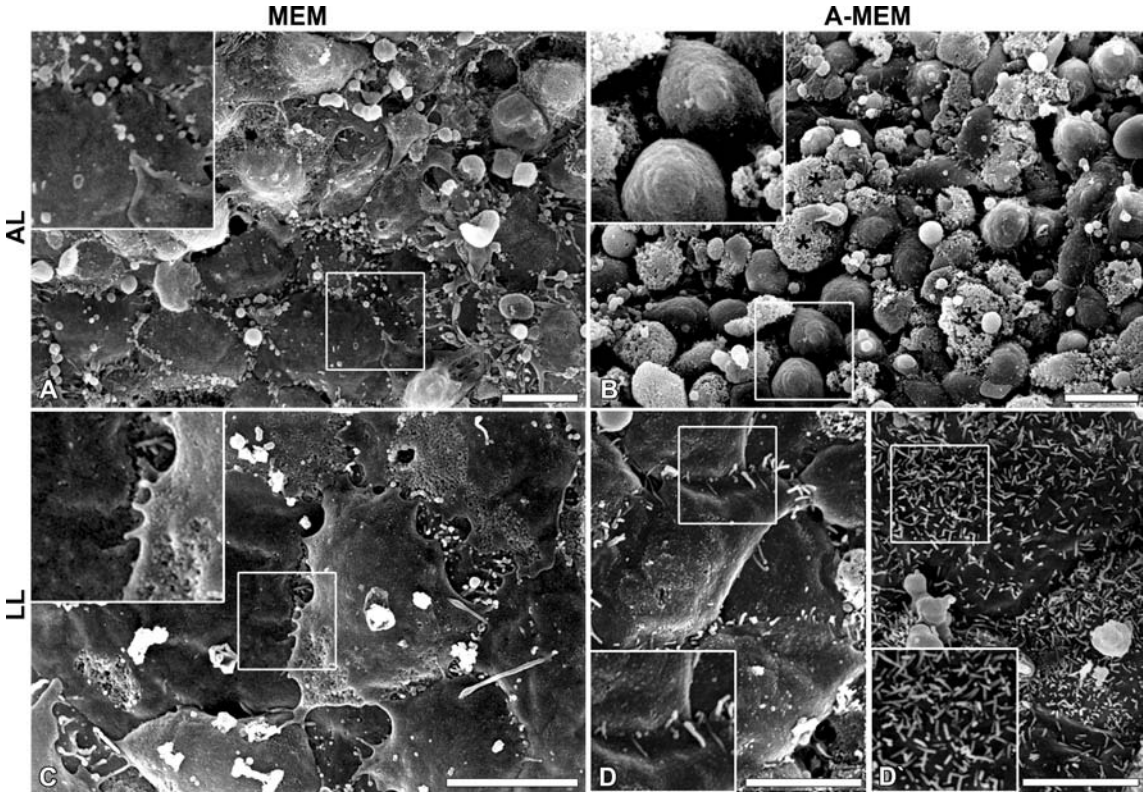

Fig. 4 Superficial RPMI 2650 cells cultured in media MEM and A-MEM at the A-L or L-L interface after 3 weeks in culture observed with SEM. (**a**, **b**) The RPMI models cultured at the AL interface exhibit squamous-like superficial cells, which do not exhibit microvilli or cilia-like structures. The cell junctions are more developed in MEM than in A-MEM. Note the necrotic superficial cells in A-MEM at the A-L interface (*). (**c**, **d**) At the L-L interface the cell junctions between the cells are more developed than at the A-L interface. In MEM the cells again developed little or no microvilli or cilia-like structures. A similar lack of developed microvilli or cilia-like structures can be seen in cells cultured in A-MEM, however occasionally such structures are visible (**D'**). Details in large white frames in **A**-**D'** are enlarged images (*two-fold*) of corresponding smaller frames. Scale bars: 10 μm.

porous membranes without cells (P_{app} 8.83×10^{-6} cm/s) was significantly higher than the permeabilities of porous membranes with seeded RPMI 2650 cells (Fig. 8a).

Jacalin Permeability of the RPMI 2650 Models

The lectin jacalin strongly binds to the tumor Thomsen-Friedenreich disaccharide antigen (Gal beta1-3GalNAc) on the cell membrane and is thus a useful membrane marker for adsorptive endocytosis. Overall, the permeability of jacalin was lower than permeability of dextran. The permeability for jacalin in RPMI 2650 models cultured in A-MEM was lower than in MEM, regardless of interface. The RPMI 2650 models cultured at the A-L interface in medium A-MEM formed the tightest barrier for jacalin (P_{app} 4.57×10^{-7} cm/s). The P_{app} of the models cultured in A-MEM at the L-L interface was similar, but slightly higher 5.72×10^{-7} cm/s. The P_{app} of the models cultured in MEM was higher and similar at both interfaces (7.20×10^{-7} cm/s at A-L and 7.36×10^{-7} cm/s at L-L) (Fig. 8b). The permeability of jacalin through the porous membranes without cells (P_{app} 9.58×10^{-6} cm/s) was significantly higher than the permeabilities of porous membranes with seeded RPMI 2650 cells (Fig. 8b).

Assessment of Fluorescently Labeled Vesicles

After 2 h of incubation, the number of dextran-labeled vesicles was the lowest in RPMI 2650 models cultured in A-MEM at the A-L interface, which corresponds to the lowest P_{app} of dextran being found in cultures in A-MEM at the A-L interface. The number of dextran-labeled vesicles was lower in models cultured at the A-L interface than at the L-L interface. The number of jacalin-labeled vesicles was however lower in cultures maintained in MEM than in A-MEM (Fig. 8c). These results might indicate a different intracellular fate of jacalin-labeled vesicles. The lower P_{app} of jacalin through the models cultured in A-MEM might correspond to higher intracellular accumulation of jacalin-labeled vesicles and higher P_{app} of jacalin through the models cultured in MEM might correspond to lower intracellular accumulation of jacalin-labeled vesicles in those models.

Drug Transporter Expression

The expression of 84 drug transporters was assessed in the RPMI 2650 cell line (Fig. 9 and Supplemental Table I). These transporters play a key role in the absorption, distribution, metabolism, and excretion of therapeutic compounds as well

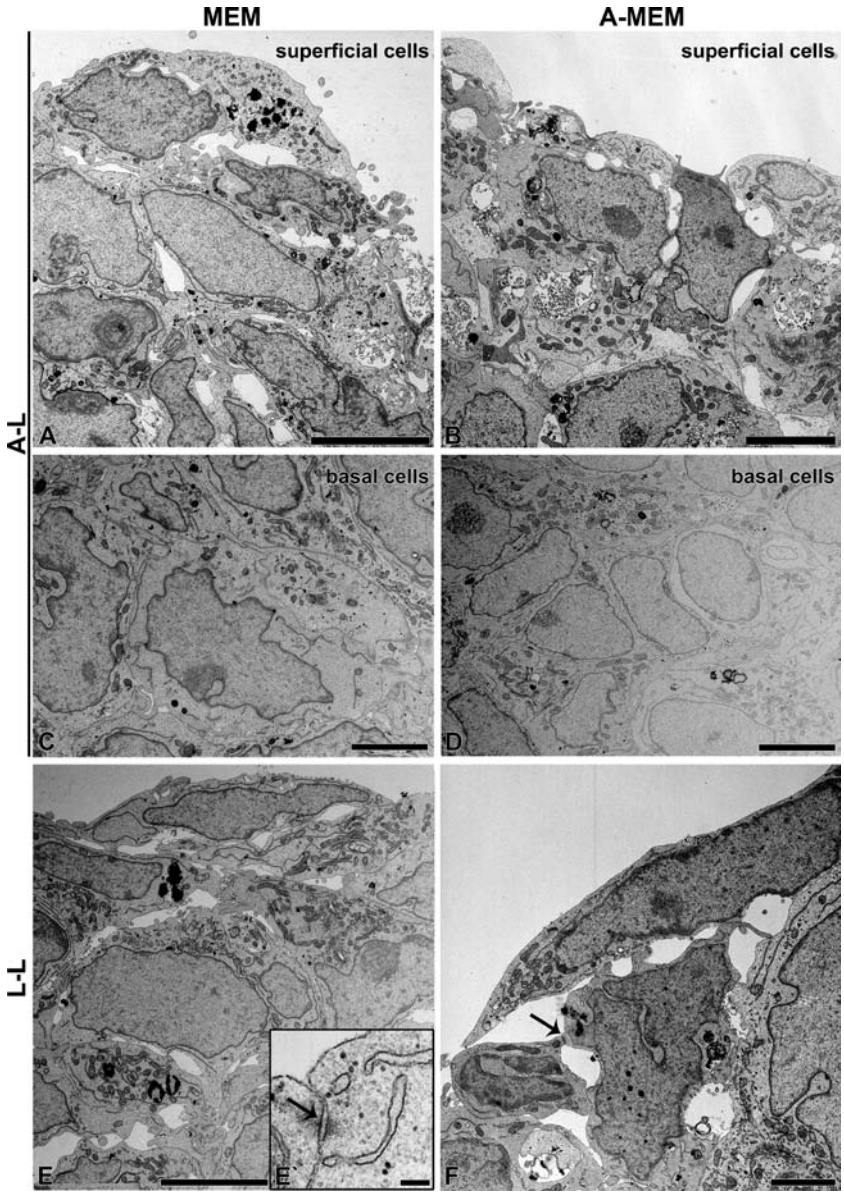

Fig. 5 RPMI 2650 epithelia cultured in media MEM and A-MEM at the A-L or L-L interface after 3 weeks in culture observed with TEM. All models exhibit large intercellular spaces in the superficial layers (**a**, **b**, **e**, **f**) and significantly smaller intercellular spaces in the basal layers (**c**, **d**). Only few or no microvilli developed in any of the four models. Cell junctions between superficial cells are overall poorly developed. Superficial cells in MEM at the L-L interface have developed desmosomes (*arrow* on **E'**); in the other models the cell junctions developed mostly between intermediate cells (*arrow* on **f**). Scale bars: **a**, **b**, **d**, **e**: 5 μm; **c**, **E'**, **f**: 2 μm.

as in the development of tumour cell resistance to chemotherapy. In Supplemental Table I we see that there is up to a 3×10^5-fold difference in gene expression between individual genes. The most expressed genes ($\Delta C_q<5$) are *ABCA4*, *ABCC1*, *ABCD3*, *ABCF1*, *ATP6V0C*, *SLC3A1*, *SLC3A2*, *SLC7A6*, *SLC7A8*, *SLC7A11*, *SLC19A2*, *SLC25A13*, *SLC38A2*, *SLCO1A2*, *VDAC1*, and *VDAC2*. Poorly expressed genes ($\Delta C_q>15$) are *ABCA9*, *ABCA13*, *ABCC12*, *SLC10A2*, *SLC15A1*, *SLC22A6*, *SLC22A7*, *SLC28A1*, *SLCO1B3*, and *SLCO2B1*.

To evaluate whether culturing conditions significantly affect gene expression, we compared four different culture conditions: the interfaces A-L and L-L and culture duration, i.e. 1 or 3 weeks. Differences larger than four-fold were considered significant and are seen in Fig. 10 Time in culture was found to be a more important factor affecting gene expression in the RPMI 2650 cell line. Prolonged culture time effected the gene expression of 12 and 7 genes at the A-L and L-L interfaces, respectively (Fig. 10a, b). Prolonged culture time increased *SLC22A2* and *SLC22A3* gene expression more than five-fold, and increased *SLC22A8* at the L-L interface, yet decreased *SLC22A8* at the A-L interface. Culturing at different interfaces affected two genes after 1 week (*AQP9* and *SLC22A8*, less expressed at L-L) and four genes after 3 weeks (*SLC22A8* was more expressed at L-L, whereas *ABCB1*, *ABCC3*, and *ABCB2* were more expressed in A-L (Fig. 10c, d).

DISCUSSION

The RPMI 2650 cell line and its culturing have not been thoroughly evaluated and so the aim of this study was to

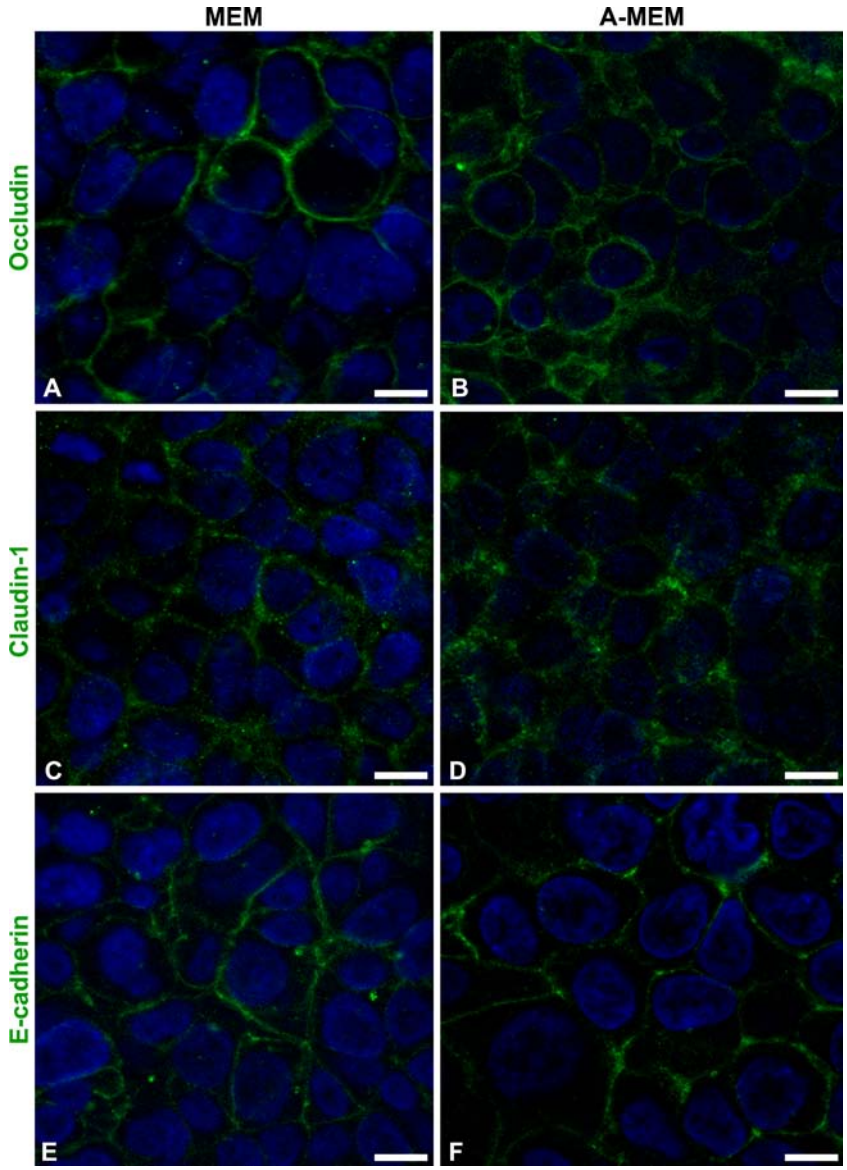

Fig. 6 Cell junction proteins of RPMI 2650 cells cultured at the L-L interface in MEM and A-MEM after 3 weeks in culture. The RPMI 2650 models at the L-L interface express occludin (**a**, **b**), claudin-1 (**c**, **d**), and E-cadherin (**e**, **f**). Scale bars: 10 μm.

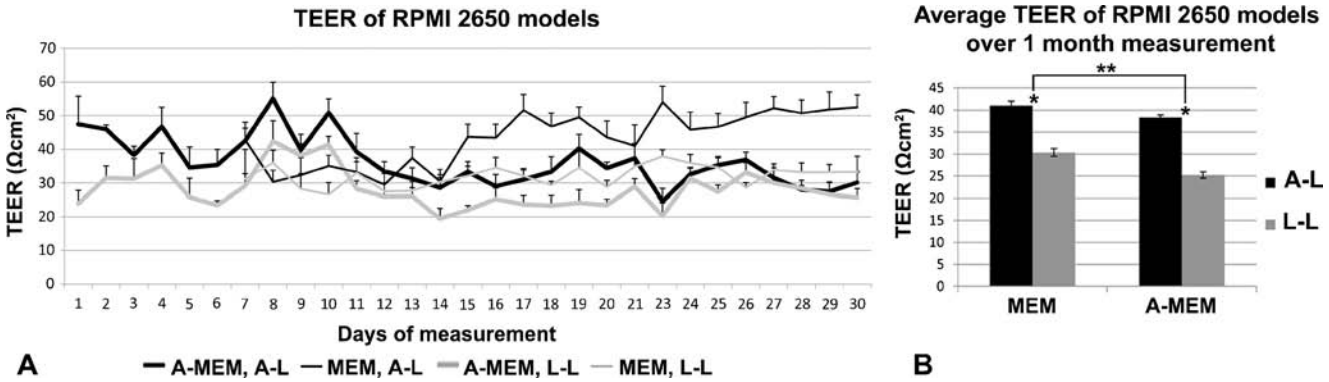

Fig. 7 TEER of different RPMI 2650 models cultured in A-MEM or MEM at the A-L or L-L interface. (**a**) The TEER measurements started when the cells reached confluence (i.e. 1 or 2 weeks after seeding). Cell cultures in A-MEM proliferated faster and thus reached confluence faster than cell cultures in MEM. Models at the A-L interface displayed consistently higher TEER than models at the L-L interface. (**b**) Mean TEER of RPMI 2650 models in media A-MEM or MEM over 1 month. The models exhibited a significantly higher mean TEER at the A-L interface (*$p < 0.05$) and when cultured in MEM medium (**$p < 0.05$).

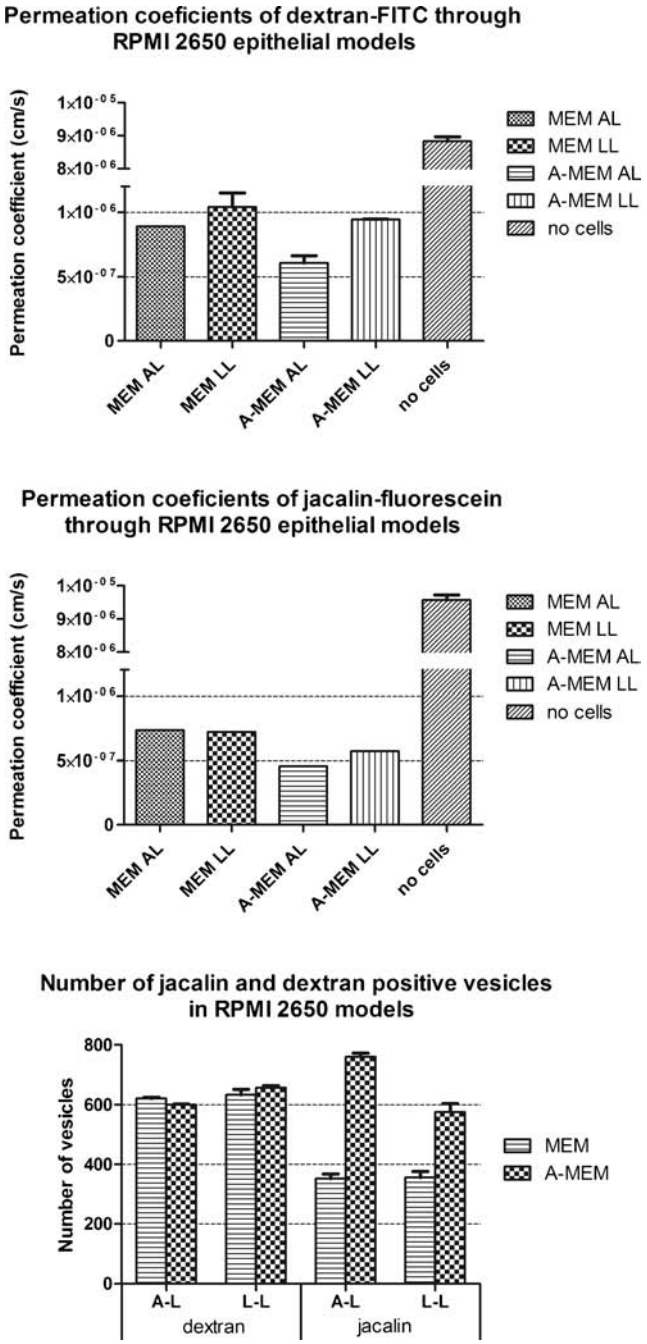

◀ **Fig. 8** Permeability of the RPMI 2650 epithelial models after 3 weeks in culture. (**a**) Dextran-FITC permeability of models cultured in A-MEM and MEM at the A-L and L-L interfaces. P_{app} of dextran is significantly higher for the cell cultures established at the L-L interface than the A-L interface. Note significantly higher P_{app} through the porous membranes without cells in comparison to poruous membranes with seeded RPMI 2650 cells. (**b**) Jacalin-fluorescein permeability of models cultured in A-MEM and MEM at the A-L and L-L interfaces. P_{app} of jacalin is comparable within each media and is in RPMI 2650 models cultured in A-MEM lower than in models cultured in MEM. Note significantly higher P_{app} through the porous membranes without cells in comparison to poruous membranes with seeded RPMI 2650 cells. (**c**) The number of jacalin- and dextran-labeled vesicles after 2 h of incubation with cells cultured in A-MEM and MEM at the A-L and L-L interfaces. The number of jacalin-labeled vesicles is significantly lower in cells cultured in MEM than in A-MEM at either interface. The number of dextran-labeled vesicles is significantly lower in cells cultured in A-MEM at the A-L interface than in all the other models (at the L-L interface, as well as in the cells cultured in MEM at the A-L and L-L interfaces.

further characterize this cell line and assess appropriate culture conditions for the optimization and standardization of a RPMI 2650 epithelial model.

After testing several seeding densities, we demonstrated the optimal seeding density at which confluence is reached in 1 week to be 6×10^5 cells/cm^2, which is similar to previous observations (9, 12). A cryopreservation method that yields maximal viability and retains cell line properties is crucial for a good standardized cell culture model. We have demonstrated that storage at both −80°C and −196°C is suitable and that the RPMI 2650 cell line retains a relatively high viability (>75%) after cryopreservation in both FBS:DMSO (9:1) and FBS:culture medium:DMSO (2:7:1). Nonetheless, the cells displayed better proliferation overall after being stored in FBS:culture medium:DMSO (2:7:1) and subsequent culture in A-MEM.

The use of A-MEM yielded higher cell proliferation than MEM in all cases and cells grown in A–MEM displayed more microvilli and cilia-like structures than in MEM. The medium A-MEM contains more amino acids, vitamins, proteins, and trace elements than MEM and already contains sodium pyruvate, which is an energy source for cells, protects against toxic hydrogen peroxide, and metabolizes amino acids. Additionally, the use of A-MEM allows the preferable cultivation of cells in reduced amounts of serum. Whereas most of the studies performed on RPMI 2650 cells used 5% or 10% serum (3, 7–9, 12, 14, 16, 18, 19), we have successfully cultured the RPMI 2650 cell line at a high proliferation rate using 2.5% FBS and suggest that the use of A-MEM for RPMI 2650 culture is superior to MEM. Cultivation at minimal amounts of serum is desirable, due to the inadequate standardization of serum. As a result of higher proliferation in A-MEM, the largest number of cell layers was achieved in models maintained in A-MEM and they also reached their highest TEER faster. The most common medium used in RPMI 2650 cell cultivation is MEM, which we tested as well and demonstrated good proliferation and viability, though slightly lower than in A-MEM. Cell viability stayed high in both media after 3 weeks in culture (>90%), suggesting the RPMI 2650 model to be most suitable for *in vitro* studies up to the third week in culture.

An additional significant factor in cell culture models is the substrate used, and Reichl and Becker demonstrated that RPMI 2650 cell cultures formed the tightest barrier on

Fig. 9 A list of the drug transporters evaluated and their gene expression in ▶ the RPMI 2650 cell line. A-L, air-liquid interface; L-L, liquid-liquid interface; 1, 1 week in culture; 3, 3 weeks in culture.

Symbol	Description	A-L1	L-L1	A-L3	L-L3
ABCA1	ATP-binding cassette, sub-family A (ABC1), member 1				
ABCA12	ATP-binding cassette, sub-family A (ABC1), member 12				
ABCA13	ATP-binding cassette, sub-family A (ABC1), member 13				
ABCA2	ATP-binding cassette, sub-family A (ABC1), member 2				
ABCA3	ATP-binding cassette, sub-family A (ABC1), member 3				
ABCA4	ATP-binding cassette, sub-family A (ABC1), member 4				
ABCA9	ATP-binding cassette, sub-family A (ABC1), member 9				
ABCB1	ATP-binding cassette, sub-family B (MDR/TAP), member 1				
ABCB11	ATP-binding cassette, sub-family B (MDR/TAP), member 11				
ABCB4	ATP-binding cassette, sub-family B (MDR/TAP), member 4				
ABCB5	ATP-binding cassette, sub-family B (MDR/TAP), member 5				
ABCB6	ATP-binding cassette, sub-family B (MDR/TAP), member 6				
ABCC1	ATP-binding cassette, sub-family C (CFTR/MRP), member 1				
ABCC10	ATP-binding cassette, sub-family C (CFTR/MRP), member 10				
ABCC11	ATP-binding cassette, sub-family C (CFTR/MRP), member 11				
ABCC12	ATP-binding cassette, sub-family C (CFTR/MRP), member 12				
ABCC2	ATP-binding cassette, sub-family C (CFTR/MRP), member 2				
ABCC3	ATP-binding cassette, sub-family C (CFTR/MRP), member 3				
ABCC4	ATP-binding cassette, sub-family C (CFTR/MRP), member 4				
ABCC5	ATP-binding cassette, sub-family C (CFTR/MRP), member 5				
ABCC6	ATP-binding cassette, sub-family C (CFTR/MRP), member 6				
ABCD1	ATP-binding cassette, sub-family D (ALD), member 1				
ABCD3	ATP-binding cassette, sub-family D (ALD), member 3				
ABCD4	ATP-binding cassette, sub-family D (ALD), member 4				
ABCF1	ATP-binding cassette, sub-family F (GCN20), member 1				
ABCG2	ATP-binding cassette, sub-family G (WHITE), member 2				
ABCG8	ATP-binding cassette, sub-family G (WHITE), member 8				
AQP1	Aquaporin 1 (Colton blood group)				
AQP7	Aquaporin 7				
AQP9	Aquaporin 9				
ATP6V0C	ATPase, H+ transporting, lysosomal 16kDa, V0 subunit c				
ATP7A	ATPase, Cu++ transporting, alpha polypeptide				
ATP7B	ATPase, Cu++ transporting, beta polypeptide				
MVP	Major vault protein				
SLC10A1	Solute carrier family 10 (sodium/bile acid cotransporter family), member 1				
SLC10A2	Solute carrier family 10 (sodium/bile acid cotransporter family), member 2				
SLC15A1	Solute carrier family 15 (oligopeptide transporter), member 1				
SLC15A2	Solute carrier family 15 (H+/peptide transporter), member 2				
SLC16A1	Solute carrier family 16, member 1 (monocarboxylic acid transporter 1)				
SLC16A2	Solute carrier family 16, member 2 (monocarboxylic acid transporter 8)				
SLC16A3	Solute carrier family 16, member 3 (monocarboxylic acid transporter 4)				
SLC19A1	Solute carrier family 19 (folate transporter), member 1				
SLC19A2	Solute carrier family 19 (thiamine transporter), member 2				
SLC19A3	Solute carrier family 19, member 3				
SLC22A1	Solute carrier family 22 (organic cation transporter), member 1				
SLC22A2	Solute carrier family 22 (organic cation transporter), member 2				
SLC22A3	Solute carrier family 22 (extraneuronal monoamine transporter), member 3				
SLC22A6	Solute carrier family 22 (organic anion transporter), member 6				
SLC22A7	Solute carrier family 22 (organic anion transporter), member 7				
SLC22A8	Solute carrier family 22 (organic anion transporter), member 8				
SLC22A9	Solute carrier family 22 (organic anion transporter), member 9				
SLC28A1	Solute carrier family 28 (sodium-coupled nucleoside transporter), member 1				
SLC28A2	Solute carrier family 28 (sodium-coupled nucleoside transporter), member 2				
SLC28A3	Solute carrier family 28 (sodium-coupled nucleoside transporter), member 3				
SLC29A1	Solute carrier family 29 (nucleoside transporters), member 1				
SLC29A2	Solute carrier family 29 (nucleoside transporters), member 2				
SLC2A1	Solute carrier family 2 (facilitated glucose transporter), member 1				
SLC2A2	Solute carrier family 2 (facilitated glucose transporter), member 2				
SLC2A3	Solute carrier family 2 (facilitated glucose transporter), member 3				
SLC31A1	Solute carrier family 31 (copper transporters), member 1				
SLC38A2	Solute carrier family 38, member 2				
SLC38A5	Solute carrier family 38, member 5				
SLC3A1	Solute carrier family 3 (cystine, dibasic and neutral amino acid transporters, activator of cystine, dibasic and neutral amino acid transport), member 1				
SLC3A2	Solute carrier family 3 (activators of dibasic and neutral amino acid transport), member 2				
SLC5A1	Solute carrier family 5 (sodium/glucose cotransporter), member 1				
SLC5A4	Solute carrier family 5 (low affinity glucose cotransporter), member 4				
SLC25A1	Solute carrier family 25, member 13 (citrin)+				
SLC7A11	Solute carrier family 7 (anionic amino acid transporter light chain, xc- system), member 11				
SLC7A5	Solute carrier family 7 (amino acid transporter light chain, L system), member 5				
SLC7A6	Solute carrier family 7 (amino acid transporter light chain, y+L system), member 6				
SLC7A7	Solute carrier family 7 (amino acid transporter light chain, y+L system), member 7				
SLC7A8	Solute carrier family 7 (amino acid transporter light chain, L system), member 8				
SLC7A9	Solute carrier family 7 (glycoprotein-associated amino acid transporter light chain, bo,+ system), member 9				
SLCO1A2	Solute carrier organic anion transporter family, member 1A2				
SLCO1B1	Solute carrier organic anion transporter family, member 1B1				
SLCO1B3	Solute carrier organic anion transporter family, member 1B3				
SLCO2A1	Solute carrier organic anion transporter family, member 2A1				
SLCO2B1	Solute carrier organic anion transporter family, member 2B1				
SLCO3A1	Solute carrier organic anion transporter family, member 3A1				
SLCO4A1	Solute carrier organic anion transporter family, member 4A1				
TAP1	Transporter 1, ATP-binding cassette, sub-family B (MDR/TAP)				
TAP2	Transporter 2, ATP-binding cassette, sub-family B (MDR/TAP)				
VDAC1	Voltage-dependent anion channel 1				
VDAC2	Voltage-dependent anion channel 2				

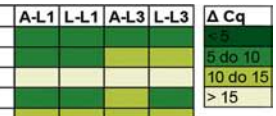

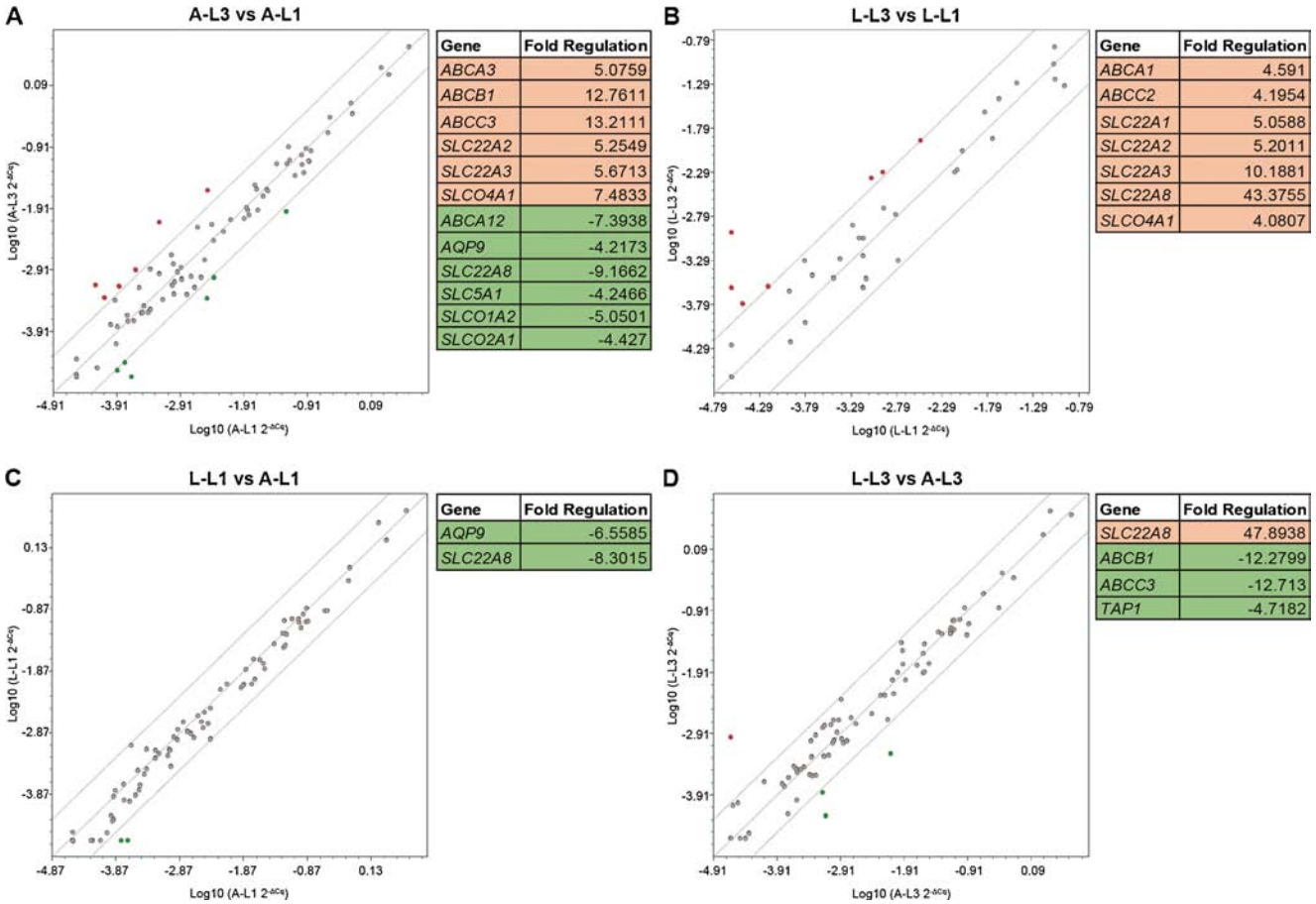

Gene	Fold Regulation
ABCA3	5.0759
ABCB1	12.7611
ABCC3	13.2111
SLC22A2	5.2549
SLC22A3	5.6713
SLCO4A1	7.4833
ABCA12	-7.3938
AQP9	-4.2173
SLC22A8	-9.1662
SLC5A1	-4.2466
SLCO1A2	-5.0501
SLCO2A1	-4.427

Gene	Fold Regulation
ABCA1	4.591
ABCC2	4.1954
SLC22A1	5.0588
SLC22A2	5.2011
SLC22A3	10.1881
SLC22A8	43.3755
SLCO4A1	4.0807

Gene	Fold Regulation
AQP9	-6.5585
SLC22A8	-8.3015

Gene	Fold Regulation
SLC22A8	47.8938
ABCB1	-12.2799
ABCC3	-12.713
TAP1	-4.7182

Fig. 10 The effect of time in culture on drug transporter gene expression in the RPMI 2650 cell line at the A-L interface (**a**) and L-L interface (**b**). Genes that are > four-fold more expressed or less expressed after 3 weeks than after 1 week are shown in *red* and *green*, respectively. The effect of the A-L or L-L interface on drug transporter gene expression in the RPMI 2650 cell line after 1 week in culture (**c**) and 3 weeks in culture (**d**). Genes that are > four-fold more or less expressed in L-L than in A-L are shown in *red* and *green*, respectively.

polyethylene terephthalate substrates (16). Therefore we tested polyethylene terephthalate porous membranes of different manufacturers and different pore size as well as on polystyrene flasks. Cell proliferation was demonstrated to be similar on all substrates, on all of which the cells formed a multi-layered epithelium. Although one study has successfully cultured the RPMI 2650 cell line as a monolayer (9), our study has demonstrated the RPMI 2650 cell line to grow in multilayers, as others have reported (3, 12, 14).

One of the key aims of *in vitro* cell models is to mimic physiological conditions as closely as possible. As a result, culturing airway epithelia at the A-L interface is preferred. To determine optimal culturing conditions for the RPMI 2650 cell line, we evaluated the effect of the A-L and L-L interface on its ability to differentiate and form a tight barrier. Unlike previous studies that failed to produce a tight epithelium of RPMI 2650 cells (7, 8), or achieved confluence only at the A-L interface (3), this study demonstrated the ability of RPMI 2650 cells to form tight cell barriers at both A-L and L-L interfaces. The models formed a multi-layered epithelium at both interfaces, with noticeably more layers (10–20) at the A-L interface, compared to 5–7 at the L-L interface. Culture in L-L resulted in less cell layers and more developed cell junctions as well as microvilli, suggesting the L-L interface to be more suitable for RPMI 2650 culture than the A-L interface. One of the possible reasons is probably that nutrients were in such a manner accessible to a multi-layered epithelium also from the apical side. Our ultrastructural examination of the models also corresponds with our TEER data, which exhibited higher mean TEER of models cultured at the A-L (38.3–41.0 Ωcm^2) than at the L-L interface (25.2–30.4 Ωcm^2). These results correspond to previous studies, which also demonstrated higher TEER of cells cultured at the A-L than at the L-L interface (3, 9). This could be the result of hyperplasia, where an increase in cell layers causes an increase in TEER (20). The thickness of the culture model is therefore a crucial factor that should be considered and controlled when we compare TEER between the various *in vitro* models. The nasal epithelium is a leaky epithelium (21–23), and excised human or animal nasal mucosa have been shown to exhibit TEER values of 40–120 Ωcm^2 (22) or 90–180 Ωcm^2 (3) and from that perspective our RPMI 2650 models resemble native nasal

mucosa regarding barrier integrity. Additionally, we have demonstrated that TEER depends on the medium used, with higher mean TEER resulting from culture in MEM.

The development of TJs in *in vitro* epithelial models is essential for drug transport studies, and so we evaluated the expression of cell junction proteins. Human nasal mucosa expresses occludin, claudin-1, −4, and −7 (4), as well as JAM-1 and ZO-1 (24). Similar to another study (9), we demonstrated the expression of occludin, claudin-1, and E-cadherin in all the models, cultured in both media A-MEM and MEM and at both A-L and L-L interfaces. The cell junction protein expression and TEER of the RPMI 2650 models is similar to that of nasal epithelium *in vivo*.

To further evaluate the barrier integrity of the RPMI 2650 models, we assessed dextran-FITC and jacalin-fluorescein permeability through all cell layers in RPMI 2650 models. In agreement with our morphological and electrophysiological evaluation of the models, the tightest barrier was formed at the A-L interface, where dextran and jacalin P_{app} were lower than at the L-L interface. Wengst and Reichl established a RPMI 2650 model with similar permeability as human nasal mucosa, with dextran FD-4 P_{app} between 24.8 and 37.7×10^{-7} cm/s (3). One more study demonstrated the 4.4 kDa dextran P_{app} to range from 93.0 to 170×10^{-7} cm/s (12). A larger 9400 MW dextran was shown to permeate rabbit nasal mucosa with a P_{app} of 6.77×10^{-7} cm/s (25), which corresponds to the permeability of dextran (MW 10000) across our RPMI 2650 models with P_{app} ranging from 6.08 to 10.04×10^{-7} cm/s. In addition to permeability analyses, we therefore also evaluated the transcytotic activity of the RPMI 2650 models by examining marker-labeled vesicles in cells. In accordance with dextran permeability of the models, the lowest number of dextran vesicles was seen in cells cultured in A-MEM at the A-L interface. Culture medium had an effect on vesicle intake and the number of jacalin-labeled vesicles was significantly lower in models cultured in MEM than in A-MEM, indicating that RPMI 2650 models respond differently to different compounds. Furthermore, in animal experiments the distinct interspecies differences must be considered very carefully when selecting the proper animal model for the permeability experiments (26). Similarly, permeability data, especially for multi-layered structures, is also required to evaluate the validity and transferability of permeability values obtained in *in vitro* experiments to clinical studies. In this regard, we should be aware that different cell layers in epithelial tissues have different permeability properties (27) and the thickness of the culture model or tissue is a crucial factor that should be considered and controlled when we compare TEER or permeability values between various *in vitro* models.

The multi-layered RPMI 2650 model in this study most closely resembles native squamous epithelium of the nasal pathway. With respect to nasal transport and metabolism studies, respiratory (pseudostratified ciliated cuboidal/columnar) epithelium is most relevant and consists of nonciliated columnar cells with microvilli, ciliated columnar cells, goblet cells with mucous granules, and basal cells (6). We have shown that RPMI 2650 cells develop microvilli, similar to previous studies (12, 15), however do not form a respiratory ciliated pseudostratified cuboidal/columnar epithelium, as has already been suggested (3).

One of the goals of developing an appropriate nasal *in vitro* model is its use in screening potential drug candidates in regard to their permeability (3). Membrane transport proteins have an important role in drug absorption (28), therefore, we tested the presence of influx and efflux drug transporters expressed in the RPMI 2650 cell line aiming to determine their expression levels and how they are affected by different culture conditions.

This study included 29 genes that encode ABC transporters. *ABCA4* predominated amongst the 7 *ABCA* genes investigated. Genes encoding the multi-drug resistant proteins (ABCB) were moderately expressed; *ABCB6* was the most abundant among them. Among the 9 multi-drug resistance-associated proteins (MRP/ABCC), *ABCC1* expression was the greatest. Functional expression of ABCC1 was previously confirmed both in RPMI 2650 cell line and in human nasal mucosa (29). In the normal human nasal respiratory mucosa ABCC1 was localized in ciliated epithelial cells and a higher level of expression was observed in serous glandular cells (30). The expression of *ABCC1* and *ABCC4* was also confirmed in rat nasal respiratory mucosa (31). In the ABCD subfamily, which includes the half transporters that are located in the peroxisome, *ABCD3* was the most abundant. One of the most expressed genes was also *ABCF1*.

Additionally, we investigated the expression of 48 genes encoding SLC transporters. Among the most abundant SLC genes were *SLC19A2*, *SLC25A1*, and *SLC38A2*. Moreover, members of the SLC3 and SLC7 families, which are amino acid transporters, were concurrently highly expressed (*SLC3A1*, *SLC3A2*, *SLC7A6*, *SLC7A8*, and *SLC7A11*). *SLC15A2* was well expressed in the RPMI 2650 cell line and its expression was previously confirmed in this cell line as well as in excised human nasal mucosa (29). Like in our study, the expression of *SLC29A1* and *SLC29A2* was relatively high also in rat nasal epithelia (31). Last but not least, *SLCO1A2* was the most abundant gene among all the organic anion transporters screened in our study.

Amongst the other transporter genes included in our study, *ATP6V0C* was highly expressed. By far the highest expressed genes were *VDAC1* and *VDAC2*. VDAC proteins in combination with anti-apoptotic proteins such as Bcl-2 and BclxL inhibit apoptosis (32), which could also be their role in RPMI 2650 cells.

The expression of some of the transporter genes was time and culture dependent (Supplemental Table I, Fig. 9). Our

results demonstrate low expression of *ABCB1* in the RPMI 2650 cell line (100-times lower than in Caco-2 cell line (internal non-published data)); however, it is time and culture dependent. The expression and functionality of *ABCB1* in the RPMI 2650 cell line has been previously verified (29) and *ABCB1* expression was also confirmed in normal mucosa of human nasal turbinates (30).

Only the expression of a few *SLC* genes was time and culture dependant and, surprisingly, they were all members of the SLC22A (organic anion transporter) subfamily. *SLC22A1*, *SLC22A2*, and *SLC22A3*, which were the most abundant among the seven *SLC22A* genes investigated, were upregulated with longer time in culture. The order of their expression was as follows: *SLC22A2* > *SLC22A3* > *SLC22A1*. The same pattern of a much higher expression of *SLC22A2* than *SLC22A3* and *SLC22A1* was observed in rat nasal epithelia (31). In contrast, Agu *et al.* reported a different expression order in cells cultured from normal and polypous human nasal tissues and concluded that *SLC22A2* is not reproducibly expressed (33). The gene, whose expression was ultimately time and culture dependent, was *SLC22A8*. However, *SLC22A8* was very poorly expressed in the RPMI 2650 cell line and its mRNA levels were elevated after 3 weeks in L-L culture conditions, and also after 1 week in A-L conditions. Furthermore, *SLCO4A1* and some other *SLCO* genes were upregulated after longer time in culture. Aquaporin-9 (AQP9) is an aquaglyceroporin membrane channel that regulates the flux of water through the membrane (34), so it is not surprising that it was downregulated in A-L conditions while it was very abundant in L-L conditions in the RPMI 2650 cell line.

To our knowledge, this is the first study to evaluate the expression of a wide range of drug transporters in the RPMI 2650 cell line and it has demonstrated that transporters of the ABC and SLC superfamilies are highly expressed. We have additionally demonstrated that culture duration significantly effects gene expression of numerous drug transporter genes. A somewhat more surprising result is that the interface at which the cells are cultured has less of an impact on drug transporter gene expression, only affecting the expression of six genes. Altered expression of drug transporters could affect the cell capacity to import and export endogenic compounds and xenobiotics and should thus be considered when designing a study using the RPMI 2650 cell line.

CONCLUSION

Culturing RPMI 2650 cells *in vitro* is simple, fast, and yields reproducible results. In this study, culture conditions have been optimized and the effects of variable culture conditions on the RPMI 2650 cell line have been demonstrated. Nevertheless, the desired characteristics of the nasal RPMI 2650 epithelial *in vitro* model should be considered when designing studies, as this study has demonstrated that different culture conditions affect cell viability, proliferation, and differentiation, epithelial morphology, barrier formation, and drug transporter expression of the cell line. The RPMI 2650 cell line is the only cell line currently in use as a nasal model and yet it still does not mimic nasal epithelium completely. Thus further research on the correlation between RPMI 2650 permeability data and *in vivo* human nasal absorption data for selected compounds is necessary to additionally clarify the suitability of the RPMI 2650 epithelial model for *in vitro* studies.

ACKNOWLEDGMENTS AND DISCLOSURES The authors thank Sanja Čabraja, Sabina Železnik, Nada Pavlica and Linda Štrus for technical assistance. The study was supported by Lek Pharmaceuticals, d.d., Sandoz Development Center Slovenia and by Slovenian Research Agency (Grants No P3-0108, P1-170).

REFERENCES

1. Ehrhardt C, Laue M, Kim K-J. *In Vitro* Models of the Alveolar Epithelial Barrier. In: Ehrhardt C, Kim K-J, editors. Drug Absorption Studies. Biotechnology: Pharmaceutical Aspects. VII: Springer US; 2008. p. 258–82.
2. Audus KL, Bartel RL, Hidalgo IJ, Borchardt RT. The use of cultured epithelial and endothelial cells for drug transport and metabolism studies. Pharm Res. 1990;7(5):435–51.
3. Wengst A, Reichl S. RPMI 2650 epithelial model and three-dimensional reconstructed human nasal mucosa as *in vitro* models for nasal permeation studies. Eur J Pharm Biopharm: Off J Arbeitsgemeinschaft fur Pharmazeutische Verfahrenstechnik eV. 2010;74(2):290–7.
4. Kamekura R, Kojima T, Koizumi J, Ogasawara N, Kurose M, Go M, *et al.* Thymic stromal lymphopoietin enhances tight-junction barrier function of human nasal epithelial cells. Cell Tissue Res. 2009;338(2):283–93.
5. Fulcher ML, Gabriel S, Burns KA, Yankaskas JR, Randell SH. Well-differentiated human airway epithelial cell cultures. Methods Mol Med. 2005;107:183–206.
6. Merkle HP, Ditzinger G, Lang SR, Peter H, Schmidt MC. *In vitro* cell models to study nasal mucosal permeability and metabolism. Adv Drug Deliv Rev. 1998;29(1–2):51–79.
7. De Fraissinette A, Brun R, Felix H, Vonderscher J, Rummelt A. Evaluation of the human cell line RPMI 2650 as an *in vitro* nasal model. Rhinology. 1995;33(4):194–8.
8. Werner U, Kissel T. In-vitro cell culture models of the nasal epithelium: a comparative histochemical investigation of their suitability for drug transport studies. Pharm Res. 1996;13(7):978–88.
9. Bai S, Yang T, Abbruscato TJ, Ahsan F. Evaluation of human nasal RPMI 2650 cells grown at an air-liquid interface as a model for nasal drug transport studies. J Pharm Sci. 2008;97(3):1165–78.
10. Moore GE, Sandberg AA. Studies of a human tumor cell line with a diploid karyotype. Cancer. 1964;17:170–5.
11. Moorhead PS. Human tumor cell line with a quasi-diploid karyotype (RPMI 2650). Exp Cell Res. 1965;39(1):190–6.
12. Kurti L, Veszelka S, Bocsik A, Ozsvari B, Puskas LG, Kittel A, *et al.* Retinoic acid and hydrocortisone strengthen the barrier function of

human RPMI 2650 cells, a model for nasal epithelial permeability. Cytotechnology. 2013;65(3):395–406.
13. Peter HG. Cell culture sheets to study nasal peptide metabolism: The human nasal RPMI 2650 cell line model. ETH Zurich: Switzerland; 1996.
14. Salib RJ, Lau LC, Howarth PH. The novel use of the human nasal epithelial cell line RPMI 2650 as an *in vitro* model to study the influence of allergens and cytokines on transforming growth factor-beta gene expression and protein release. Clin Exp Allergy: J Br Soc Allergy Clin Immunol. 2005;35(6):811–9.
15. Ding GQ, Zheng CQ, Liu Y, Tian J. Roles of epidermal growth factor receptor signaling pathway on cultured human nasal epithelial cells RPMI-2650. Zhonghua er bi yan hou tou jing wai ke za zhi. Chin J Otorhinolaryngol Head Neck Surg. 2009;44(3):203–8.
16. Reichl S, Becker K. Cultivation of RPMI 2650 cells as an in-vitro model for human transmucosal nasal drug absorption studies: optimization of selected culture conditions. J Pharm Pharmacol. 2012;64(11):1621–30.
17. Carr SF, Papp E, Wu JC, Natsumeda Y. Characterization of human type I and type II IMP dehydrogenases. J Biol Chem. 1993;268(36): 27286–90.
18. Keenan J, Liang Y, Clynes M. Two-deoxyglucose as an anti-metabolite in human carcinoma cell line RPMI-2650 and drug-resistant variants. Anticancer Res. 2004;24(2A):433–40.
19. Wilkinson LJ, Duffield ML, Titball RW, Lindsay CD. Down-regulation of gene transcripts associated with ricin tolerance in human RPMI 2650 cells. Toxicol in vitro: Int J Publ Assoc BIBRA. 2007;21(3):509–20.
20. Visnjar T, Kreft ME. Air-liquid and liquid-liquid interfaces influence the formation of the urothelial permeability barrier *in vitro*. In Vitro Cell Dev Biol Anim. 2013;49(3):196–204.
21. Campbell ML, Abboud EC, Dolberg ME, Sanchez JE, Marcet JE, Rasheid SH. Treatment of refractory perianal fistulas with ligation of the intersphincteric fistula tract: preliminary results. Am Surg. 2013;79(7):723–7.
22. Schmidt MC. Therapeutic peptides: How Do they Get through the nasal epithelium? ETH Zurich: Switzerland; 1999.
23. Hosoya K, Kubo H, Natsume H, Sugibayashi K, Morimoto Y, Yamashita S. The structural barrier of absorptive mucosae: site difference of the permeability of fluorescein isothiocyanate-labelled dextran in rabbits. Biopharm Drug Dispos. 1993;14(8):685–95.
24. Takano K, Kojima T, Go M, Murata M, Ichimiya S, Himi T, *et al.* HLA-DR- and CD11c-positive dendritic cells penetrate beyond well-developed epithelial tight junctions in human nasal mucosa of allergic rhinitis. J Histochem Cytochem: Off J Histochem Soc. 2005;53(5): 611–9.
25. Kubo H, Hosoya K-I, Natsume H, Sugibayashi K, Morimoto Y. *In vitro* permeation of several model drugs across rabbit nasal mucosa. Int J Pharm. 1994;103(1):27–36.
26. Loch C, Zakelj S, Kristl A, Nagel S, Guthoff R, Weitschies W, *et al.* Determination of permeability coefficients of ophthalmic drugs through different layers of porcine, rabbit and bovine eyes. Eur J Pharm Sci: Off J Eur Fed Pharm Sci. 2012;47(1):131–8.
27. Kreft ME, Hudoklin S, Jezernik K, Romih R. Formation and maintenance of blood-urine barrier in urothelium. Protoplasma. 2010;246 (1–4):3–14.
28. Bosquillon C. Drug transporters in the lung–do they play a role in the biopharmaceutics of inhaled drugs? J Pharm Sci. 2010;99(5):2240–55.
29. Reichl S, Dolberg A. Expression analysis of drug transporter proteins in RPMI 2650 cell line and excised human nasal mucosa. AAPS 2013 Annual Meeting & Exposition; November 10–14 2013; Henry B. Gonzales Convention Center, San Antonio, TX, USA 2013.
30. Wioland MA, Fleury-Feith J, Corlieu P, Commo F, Monceaux G, Lacau-St-Guily J, *et al.* CFTR, MDR1, and MRP1 immunolocalization in normal human nasal respiratory mucosa. J Histochem Cytochem: Off J Histochem Soc. 2000;48(9):1215–22.
31. Genter MB, Krishan M, Augustine LM, Cherrington NJ. Drug transporter expression and localization in rat nasal respiratory and olfactory mucosa and olfactory bulb. Drug Metab Dispos: Biol fate Chem. 2010;38(10):1644–7.
32. Leanza L, Biasutto L, Manago A, Gulbins E, Zoratti M, Szabo I. Intracellular ion channels and cancer. Front Physiol. 2013;4:227.
33. Agu R, MacDonald C, Cowley E, Shao D, Renton K, Clarke DB, *et al.* Differential expression of organic cation transporters in normal and polyps human nasal epithelium: implications for *in vitro* drug delivery studies. Int J Pharm. 2011;406(1–2):49–54.
34. Karlsson T, Bolshakova A, Magalhaes MA, Loitto VM, Magnusson KE. Fluxes of water through aquaporin 9 weaken membrane-cytoskeleton anchorage and promote formation of membrane protrusions. PLoS ONE. 2013;8(4):e59901.